

A Hybrid Framework for Topology Identification of Distribution Grid With Renewables Integration

Xing He , Member, IEEE, Robert C. Qiu , Fellow, IEEE, Qian Ai , Senior Member, IEEE, and Tianyi Zhu

Abstract—Topology identification (TI) is a key task for state estimation (SE) in distribution grids, especially the one with high-penetration renewables. The uncertainties, initiated by the time-series behavior of renewables, will *almost certainly* lead to bad TI results *without a proper treatment*. These uncertainties are *analytically intractable* under conventional framework—they are usually *jointly spatial-temporal dependent*, and hence cannot be simply treated as white noise. For this purpose, a hybrid framework is suggested in this paper to handle these uncertainties in a *systematic and theoretical* way; in particular, big data analytics are studied to *harness the jointly spatial-temporal statistical properties* of those uncertainties. With some prior knowledge, a model bank is built first to store the *countable* typical models of network configurations; therefore, the difference between the SE outputs of each bank model and our observation is *capable of being defined as a matrix variate*—the so-called *random matrix*. In order to gain insight into the random matrix, a *well-designed metric space* is needed. Auto-regression (AR) model, factor analysis (FA), and random matrix theory (RMT) are tied together for the metric space design, followed by *jointly temporal-spatial analysis* of those matrices which is conducted in a *high-dimensional (vector) space*. Under the proposed framework, some *big data analytics and theoretical results* are obtained to improve the TI performance. Our framework is validated using IEEE standard distribution network with some field data in practice.

Index Terms—Topology identification, renewables, uncertainty, random matrix theory, AR model, factor analysis, high dimension.

I. INTRODUCTION

TOPOLOGY identification (TI) of admittance matrix \mathbf{Y} , the so-called network topology, is a precondition for state estimation (SE) in distribution systems. Inaccurate TI has long been cited as a major cause of bad SE results [1]. During a daily operation, \mathbf{Y} may be partially reconfigured [2]. While the knowledge of \mathbf{Y} is crucial, it may be unavailable or outdated (via TI) due to some reasons [3]–[7]. Among these reasons, the uncertainties caused by the behavior of high-penetration renewables

Manuscript received March 5, 2020; revised July 22, 2020; accepted September 13, 2020. Date of publication September 18, 2020; date of current version February 19, 2021. This work was in part supported by the National Key Research & Development (R&D) plan of China under Grant 2016YFB0901300, and in part by National Natural Science Foundation of China under Grants 51907121 and U1866206. Paper no. TPWRS-00350-2020. (Corresponding author: Qian Ai.)

Xing He, Qian Ai, and Tianyi Zhu are with the Department of Electrical Engineering, Shanghai Jiaotong University, Shanghai 200240, China (e-mail: hexing_hx@126.com; aiqian@sjtu.edu.cn; zty0912@sjtu.edu.cn).

Robert C. Qiu is with the Electrical Engineering and Computer Engineering, Tennessee Technological University, Cookeville, TN 38505 USA (e-mail: rqiu@ieee.org).

Color versions of one or more of the figures in this article are available online at <https://ieeexplore.ieee.org>.

Digital Object Identifier 10.1109/TPWRS.2020.3024955

[8], [9], which are analytically intractable for most tools, are one of the main challenges. How to address these uncertainties by harnessing their jointly spatial-temporal statistical properties is at the heart of our study, and this question threads throughout the proposed hybrid framework.

A. Related Work and Motivation of our Work

Ref. [10]–[12] are relevant to our paper to an extent. Ref. [10] builds a model bank, and then conducts TI task by applying a recursive Bayesian approach to identify the correct network configuration in the bank. Ref. [11] conducts TI task by comparing the collected voltage time-series with a library of signatures computed a priori. Ref. [12] formulates the TI problem as a mixed integer quadratic programming (MIQP) model to find a topology configuration with weighted least square (WLS) of measurement residues.

Several data-driven TI approaches, as Ref. [3]–[7], are proposed recently. They are mainly based on iterations, graph theory, sparsity-based regularization, and so on. These approaches are feasible to TI task with very little knowledge about the network. Ref. [6] tells that an accurate TI result is acquirable only if the noise is well addressed. For instance, even with a small error in measurements, the regression-based method may fail in TI task (see Section V-C in *Case Studies*). Most TI algorithms, especially those derived from least square, rely heavily on the second-order statistics of meter data [4], [5], and hence they are applicable to (Gaussian) white noise.

Renewables-derived uncertainties (e.g., randomness caused by a gust of wind), however, often exhibit themselves as non-Gaussian noise. The conventional statistics such as first/second-order statistics (mean/variance) are even not nearly enough to represent these non-Gaussian variables, and the (jointly spatial-temporal) dependence should be taken into account. Therefore, there is an urgent need for some powerful approach to make these uncertainties analytically tractable with a systematic and theoretical procedure. This is the major motivation and superiority of our proposed hybrid framework. Under our framework, some statistical properties and theoretical results are established.

B. Our Work and its Contributions

In order to handle the renewables-derived uncertainties, we have to go back to the model bank following Ref. [10], [11]. It is reasonable and feasible to list all the possible models in practice with prior knowledge, since the network configuration

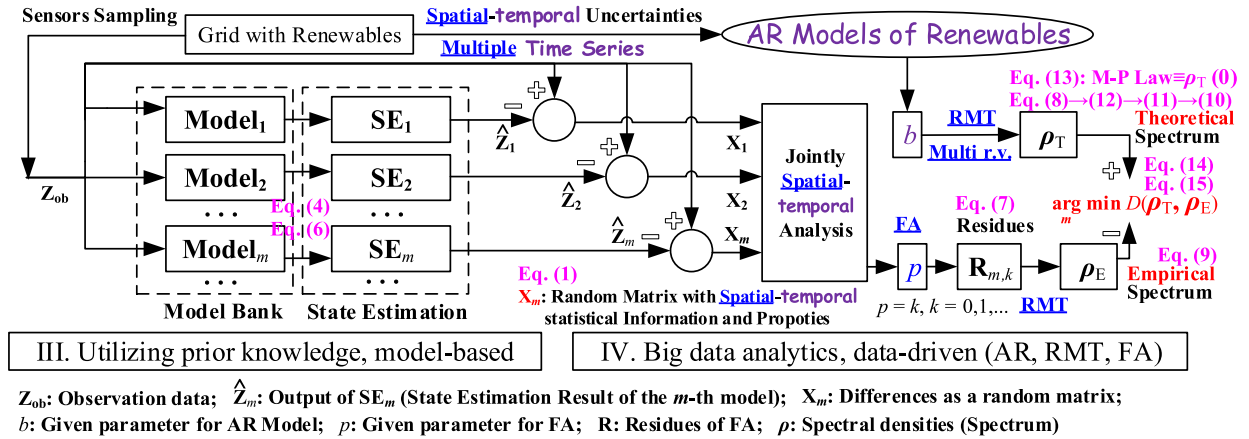


Fig. 1. Proposed Hybrid Framework.

of a particular grid must be confined to only a few typical models. Because of the bank, the difference between the bank model SE output and our observation is capable of being defined as a matrix variate—the so-called random matrix.

Then we move to the heart of our hybrid framework—high-dimensional analytics of the random matrix. Auto-regression (AR) model, factor analysis (FA), and random matrix theory (RMT) are tied together for the jointly temporal-spatial modeling and analysis of the random matrices. And high-dimensional statistics are obtained as big data analytics. This framework enables us to gain insight into the (multiple) renewables-derived uncertainties, which are analytically intractable under conventional framework.

In particular, our framework deals with a large number (spatial space, N) of nodes simultaneously, and each node ($i = 1, \dots, N$) samples time-series within a given duration (temporal space, T) of observation. Classical statistic theories treat fixed N only (often small, typically $N < 6$ [13]). This fixed (small) N is called the low-dimensional regime. In practice, we are interested in the case that N can vary arbitrarily in size compared with T (often T is large, typically $N > 20$, $c = N/T > 0$ [13]). This fundamental requirement is the primary driving force for us to study big data analytics with high-dimensional statistics. For jointly spatial-temporal analysis, a (large-dimensional) data matrix, rather than a vector or a scalar [14], is adopted as the basis.

This work is expected to contribute some insight to the renewables-derived uncertainties that are often analytically intractable. We take advantage of high-dimensional statistics that is made analytically tractable only recently [15], [16]. To our knowledge, this type of analysis is, for the first time, conducted in the context of TI. Our big data analytics are motivated to improve TI performance, and may be further expanded to other applying fields: the detection and localization of faults [17], the detection of unmonitored switching of circuit breakers in network reconfiguration [18], etc.

The remainder of this paper is organized as follows.

- 1) Section II presents the hybrid framework and gives a general discussion about it.

- 2) Section III, by employing the model bank, aims to convert our observation into a random matrix with prior knowledge.
- 3) Section IV studies the high-dimensional statistics of the random matrices based on AR, FA, and RMT.
- 4) Section V validates our framework with case studies based on IEEE standard distribution network using some field data.

II. HYBRID FRAMEWORK OF TOPOLOGY IDENTIFICATION

A. Hybrid Framework

Fig. 1 summarizes the presented framework by illustrating how Model Bank, AR, FA, RMT are put together coherently. The hybrid framework mainly consists of two parts—the model-based part (Section III) and the data-driven part (Section IV). The former, with prior knowledge, converts the observed data into “difference” in the form of random matrix. Starting from the random matrix and going through a rigorous mathematic procedure, the latter aims to gain insight into the uncertainties through big data analytics, with a focus on the jointly spatial-temporal analysis and the underlying theories/tools.

First, we build “bank” (referring to [10]) to store countable (often a few) virtual models mapping the possible network configurations of a real grid. The bank can be seen as the universal set of possible models among which we try to pick out the most likely one. Hence, we need a well-designed metric space—a set together with a metric defined on it.

The SE for the models, mainly based on power flow (PF) analysis, is the second step. We make an assumption that each agent on distributed nodes (Agent i on Node i for instance) does collect some local information, such as power usage (P_i) and voltage magnitude (V_i), on its own access point (Node i). However, it has no prior information about how it is connected via power lines in the network, not to mention power flow on the branch ($P_{i,j}$ and $Q_{i,j}$). The information on $P_{i,j}$ and $Q_{i,j}$ is often a precondition for some SE algorithms [12], but not for ours. From this aspect, our assumption is practical and flexible for engineering scenarios.

Then we move forwards to the difference \mathbf{X} , which is modeled as a non-Gaussian random matrix for further big data analytics. For each bank model (Model M_m for instance), its SE output ($\hat{\mathbf{Z}}_m$) does provide a comparison for our observation (\mathbf{Z}_{ob}), and then the difference \mathbf{X}_m is defined as

$$\mathbf{X}_m = \mathbf{Z}_{\text{ob}} - \hat{\mathbf{Z}}_m. \quad (1)$$

Each \mathbf{X}_m consists of multiple time-series, which can be generally decomposed into four components—the trend, the seasonality, the mutation, and the randomness. Feature extraction of the trend and the seasonality is a well discussed topic in time-series analysis [19], and our previous work [20] has proposed an RMT-based mutation detection algorithm to handle sudden changes. Here we focus on the randomness.

B. Non-Gaussian Randomness Tools and Related Work

The randomness component of renewables-derived uncertainties cannot be simply modeled as white noise—successive observed data in the form of time-series usually show serial dependence. In order to formally incorporate this (*temporal*) dependent structure, it is reasonable to explore a general class of models called auto-regressive (AR) models— $x_t = \sum_{i=1}^p b_i x_{t-1} + \epsilon_t$ [21]. From the *spatial* aspect, FA and RMT are tied together to conduct jointly temporal-spatial analysis of the dependence among those multiple time-series.

- 1) Factor Analysis: FA is often used for dimension reduction in high-dimensional datasets [15]. Because of the latent constructs (e.g., spatial-temporal independence) lying in the sampling data, FA is preferred to principal component analysis (PCA) [22]. FA has already been successfully applied in various fields such as statistics [23] and econometrics [24]. Ref. [25] employs FA to handle high-frequency data in financial market. In power system domain, our previous work [26] applies FA to anomaly detection and location with both simulated data and field data.
- 2) Random Matrix Theory: The entries of a random matrix are random variables and the matrix size is often very large, so RMT is naturally connected with our problem at hand. The goal of RMT is to understand the joint eigenvalue distribution in the asymptotic regime as the statistic analytics from big data. To our best knowledge, RMT is developed to address this high-dimensional regime since classical statistic theories apply to low-dimensional regime only [13]. Recently, RMT has already been successfully applied in many fields of power system [20].
- 3) ARMA+RMT: This mode is relevant to our big data analytics. Ref. [27] employs the free random variables (FRV) calculus to calculate the empirical spectral density (ESD) of the sample covariance for several VARMA-type processes. The derivation is RMT-based and mathematically rigorous; the theoretical result is nicely matched against the spectra obtained via Monte Carlo simulations.

III. MODEL-BASED PART UTILIZING PRIOR KNOWLEDGE

This part aims to convert our observed data into “difference” in the form of random matrices. With PF analysis, the SE output

of each bank model is computed as \mathbf{Z}_m . It supplies a comparison for our observed data \mathbf{Z}_{ob} , and hence the difference is capable of being defined (Eq. 1).

A. Grid Network Operation

For each node in a power grid, Node i for instance, considering the node-to-ground admittance y_i ($y_i = g_i + j \cdot b_i$, $j = \sqrt{-1}$), its active power P and reactive power Q are expressed as:

$$\begin{cases} P_i = V_i \sum_{k \neq i} V_k (G_{ik} \cos \theta_{ik} + B_{ik} \sin \theta_{ik}) - V_i^2 \sum_{k \neq i} G_{ik} - V_i^2 g_i \\ Q_i = V_i \sum_{k \neq i} V_k (G_{ik} \sin \theta_{ik} - B_{ik} \cos \theta_{ik}) + V_i^2 \sum_{k \neq i} B_{ik} + V_i^2 b_i \end{cases} \quad (2)$$

Abstractly, a physical power system obeying Eq. (2) can be viewed as an analog engine—it takes bus voltage magnitude V and phase angel θ as inputs, conductance G and susceptance B as given parameters, and “computes” active power injection P and reactive power injection Q as outputs. Thus, the entries of Jacobian matrix \mathbf{J} , i.e. $[J]_{ij}$, are defined as the partial derivatives of the outputs, P and Q , with respect to the inputs, V and θ . All in all, \mathbf{J} consists of four parts \mathbf{H} , \mathbf{N} , \mathbf{K} , \mathbf{L} :

$$\begin{cases} H_{ij} = V_i V_j (G_{ij} \sin \theta_{ij} - B_{ij} \cos \theta_{ij}) - \delta_{ij} \cdot Q_i + \delta_{ij} \cdot V_i^2 b_i \\ N_{ij} = V_i V_j (G_{ij} \cos \theta_{ij} + B_{ij} \sin \theta_{ij}) + \delta_{ij} \cdot P_i - \delta_{ij} \cdot V_i^2 g_i \\ K_{ij} = -V_i V_j (G_{ij} \cos \theta_{ij} + B_{ij} \sin \theta_{ij}) + \delta_{ij} \cdot P_i + \delta_{ij} \cdot V_i^2 g_i \\ L_{ij} = V_i V_j (G_{ij} \sin \theta_{ij} - B_{ij} \cos \theta_{ij}) + \delta_{ij} \cdot Q_i + \delta_{ij} \cdot V_i^2 b_i \end{cases} \quad (3)$$

where $H_{ij} = \frac{\partial P_i}{\partial \theta_j}$, $N_{ij} = \frac{\partial P_i}{\partial V_j} V_j$, $K_{ij} = \frac{\partial Q_i}{\partial \theta_j}$, $L_{ij} = \frac{\partial Q_i}{\partial V_j} V_j$.

B. Power Flow Analysis

PF analysis deals mainly with the calculation of steady-state system status, i.e., voltage magnitude V and phase angel θ , on each network bus, for a given set of variables such as load demands, under certain assumptions such as in a balanced system operation [28]. Conventional PF analysis is model- and assumption-based. That is to say, the information of network topology \mathbf{Y} is a prerequisite for the calculation, and the input (output) variables need to be preset as one of the following three categories:

- P and V (Q and θ) for voltage controlled bus/PV bus;
- P and Q (V and θ) for load bus/PQ bus;
- V and θ (P and Q) for reference bus/slack bus.

Consider a power system with n buses, among which there are m PV buses, l PQ buses, and 1 slack bus ($n = l + m + 1$). Starting with Eq. (2), PF functions is formulated as Eq. (4).

$$\mathbf{y} := \begin{bmatrix} P_1 \\ \vdots \\ P_{n-1} \\ Q_{m+1} \\ \vdots \\ Q_{n-1} \end{bmatrix} = \mathbf{f} \begin{bmatrix} \theta_1 \\ \vdots \\ \theta_{n-1} \\ V_{m+1} \\ \vdots \\ V_{n-1} \end{bmatrix} =: \mathbf{f}(\mathbf{x}) \quad \mathbf{J} = \begin{bmatrix} \frac{\partial y_1}{\partial x_1} & \dots & \frac{\partial y_1}{\partial x_K} \\ \vdots & \ddots & \vdots \\ \frac{\partial y_K}{\partial x_1} & \dots & \frac{\partial y_K}{\partial x_K} \end{bmatrix} \quad (4)$$

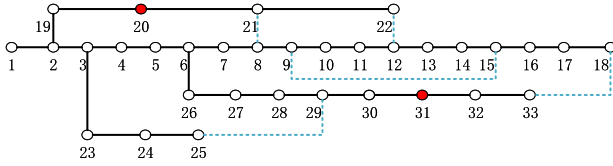


Fig. 2. IEEE 33-bus Network

where $:=$ is the assignment symbol in computer science.

Eq. (4) builds a differentiable mapping function $\mathbf{f}: \mathbf{x} \in \mathbb{R}^K \rightarrow \mathbf{y} \in \mathbb{R}^K$. It consists of $K = 2n - m - 2$ equations, from the same number ($m + 2l = K$) state variables, θ and V , to the power injections, P and Q . Following Eq. (3), \mathbf{J} is calculated as a $K \times K$ matrix:

$$\mathbf{J} = \begin{bmatrix} [\mathbf{H}]_{n-1, n-1} & [\mathbf{N}]_{n-1, n-m-1} \\ [\mathbf{K}]_{n-m-1, n-1} & [\mathbf{L}]_{n-m-1, n-m-1} \end{bmatrix} \quad (5)$$

To formulate the linear approximation process that the system operation point shifts from $(\mathbf{x}^{(k)}, \mathbf{y}^{(k)})$ to $(\mathbf{x}^{(k+1)}, \mathbf{y}^{(k+1)})$, the iteration is set as follows:

$$\mathbf{x}^{(k+1)} := \mathbf{x}^{(k)} + \mathbf{J}^{-1} \left(\mathbf{x}^{(k)} \right) \left(\mathbf{y}^{(k+1)} - \mathbf{y}^{(k)} \right) \quad (6)$$

The iteration depicts how to update the state variables from $\mathbf{x}^{(k)}$ to $\mathbf{x}^{(k+1)}$. $\mathbf{y}^{(k)}$ and $\mathbf{x}^{(k)}$ are known quantities under our assumption in Section II-A. $\mathbf{y}^{(k+1)}$, according to Eq. (4), is the desired P, Q on PQ buses and desired P on PV buses¹. $\mathbf{x}^{(k+1)}$ is the state variables that need to be estimated through the iteration in this expression (Eq. 6).

The above model-based deterministic PF analysis is not always reliable in practice, since the network topology \mathbf{Y} , and the operation points $(\mathbf{x}^{(k)}, \mathbf{y}^{(k)})$ are required to be of high precision and up-to-date. These requirements, unfortunately, are often unrealistic as mentioned in Sec I.

C. Model Bank

During the daily operation of a distribution grid, its topology may be partially reconfigured due to maintenance or emergency/optimal operation. Taking IEEE 33-bus network for instance, the network topology is shown in Fig. 2. It is a 12.66-kV distribution grid system including a substation and 37 branches. The normally closed branches are represented by solid lines, and normally opened ones by dashed lines.

With the pair switch of these normally closed/opened branches, the grid has ‘countable’ possible network configurations. In practice, however, it is reasonable to study only a few models even for a large system, since the network configuration of a particular grid must be confined to several typical models. We employ the concept of ‘bank’ referring to [10] to store them, and the deterministic PF analysis works out the SE results of these models as $\hat{\mathbf{Z}}_m$. These SE outputs $\hat{\mathbf{Z}}_m$ allow of the comparison with our observed data \mathbf{Z}_{ob} , and hence the difference \mathbf{X} is capable of being defined as a random matrix (Eq. 1). In this way, the TI task is converted into a matching problem under

¹For PQ buses, neither V nor θ are fixed; they are state variables that need to be estimated. For PV buses, V is fixed, and θ needs to be estimated.

certain metric space. The design of the metric space will be discussed in Section IV-E.

IV. HIGH-DIMENSIONAL ANALYSIS WITH RMT AND FA

Our motivation arises from the fact that the renewables-derived uncertainties cannot be simply modeled as white noise. They do contain much (latent) structural information, especially when there is an extra bias caused by a certain (although maybe unknown) poor assumption or negligence. For this purpose, FA is employed in our framework. The entries of the resultant matrix are random variables in large size, so RMT is naturally relevant to the problem [20].

A. RMT-Based Problem Formulation

The goal of RMT is to understand joint eigenvalue distribution in the asymptotic regime as big data analytics. The spectrum of a covariance matrix generally consists of two parts: A few spikes/outliers and the bulk. The former represents common factors that mainly drive the features, and the latter represents unique factors or error variation that arise from idiosyncratic noise. For the noise part, we consider a minimum distance between two spectral densities—a *theoretical* one ρ_T from an ideal structure model, and an empirical one ρ_E relevant to the (multiple time-series) observed data.

B. Factor Analysis Formula

To deal with high-dimensional datasets, FA is often used for dimension reduction in sampling data with underlying constructs that cannot be measured directly [15], [22].

Regarding empirical data $\mathbf{X} \in \mathbb{R}^{N \times T}$, FA is formulated as

$$\mathbf{X} = \mathbf{L}^{(p)} \mathbf{F}^{(p)} + \mathbf{R}. \quad (7)$$

where $\mathbf{F} \in \mathbb{R}^{p \times T}$ is a matrix of common factors, $\mathbf{L} \in \mathbb{R}^{N \times p}$ is factor loadings, p is factor numbers, and $\mathbf{R} \in \mathbb{R}^{N \times T}$ is residues, also called unique factors or error variation.

Eq. (7) enables to decompose observed data \mathbf{X} into systematic information and idiosyncratic noise. Usually, only \mathbf{X} is observable, \mathbf{L} is composed of the first p principal components of \mathbf{X} , $\mathbf{F} = (\mathbf{L}^T \mathbf{L})^{-1} \mathbf{L}^T \mathbf{X}$, and $\mathbf{R} = \mathbf{X} - \mathbf{L} \mathbf{F}$.

We focus on residues \mathbf{R} , which may contain some latent constructs and statistical information. Instead of regarding \mathbf{R} as Gaussian noise a priori, we assume that there are cross- and auto-correlated structures. Without loss of generality, $\hat{\mathbf{R}}$ is represented as

$$\hat{\mathbf{R}} = \mathbf{A}_N^{1/2} \boldsymbol{\epsilon} \mathbf{B}_T^{1/2} \quad (8)$$

where $\boldsymbol{\epsilon}$ is an $N \times T$ Gaussian matrix with independent and identically distributed (i.i.d.) random entries, \mathbf{A}_N and \mathbf{B}_T are $N \times N$ and $T \times T$ symmetric non-negative definite matrices, representing cross- and auto- covariances, respectively. Eq. (8) leads to a separable sample covariance matrix in the sense that \mathbf{A}_N and \mathbf{B}_T are separable. This structural assumption of separability is a popular assumption in the analysis of spatial-temporal data [16]. Although this assumption does not allow for spatial-temporal interactions in the covariance matrix, in many real data

applications, the covariance matrix can be well approximated using separable covariance matrices for a space-time covariance matrix problem.

C. FA Estimation Based on Spectrum Analysis

Now the objective of the mentioned matching problem is to match the spectral density ρ_E against ρ_T .

The former ρ_E means the ESD of the covariance matrix of residues \mathbf{R} constructed from empirical data. It can be controlled by the p number of common factors to be removed following Eq. (7). It is defined as [29]

$$\rho_E(\lambda) = \frac{1}{N} \sum_{i=1}^N \delta(\lambda - \lambda_i^{(C_N)}) \quad (9)$$

where $\{\lambda_i^{(C_N)}\}_{i=1}^N$ is the eigenvalues of $\mathbf{C}_N = \frac{1}{T} \mathbf{R} \mathbf{R}^T$, and δ is the Dirac delta function.

The latter ρ_T means the theoretical spectral density of the ideal covariance matrix $\hat{\mathbf{C}}_N$ with the assumed structural model, i.e., $\hat{\mathbf{C}}_N = \frac{1}{T} \hat{\mathbf{R}} \hat{\mathbf{R}}^T = \frac{1}{T} \mathbf{A}_N^{1/2} \epsilon \mathbf{B}_T \epsilon^T \mathbf{A}_N^{1/2}$ (Eq. 8). Assuming a parsimonious matrix structure of \mathbf{A}_N and \mathbf{B}_T , which is determined by only a small parameter set θ . Mathematically motivated by the result of [30], the spectral density of $\hat{\mathbf{C}}_N$, under certain assumptions, converges to a certain limiting distribution $\rho_T(\theta)$, as the size N tends to infinity.

D. Simplified Model on Covariance Structures of Residues

A difficulty lies in the calculation of the limiting density, $\rho_T(\theta)$, for general $\theta = (\theta_{\mathbf{A}_N}, \theta_{\mathbf{B}_T})$. The actual calculation of $\rho_T(\theta)$ is quite complex, which makes the implementation difficult. A recent study of [27], fortunately, provides the direct derivation of this limiting spectral density using free random variable (FRV) techniques. They particularly present analytic forms when the time-series data follow ARMA processes. In our task, we employ these techniques to calculate $\rho_T(\theta)$. First, two assumptions are made:

- I. The cross-correlations of $\hat{\mathbf{R}}$ are effectively eliminated by removing p factors, and therefore $\hat{\mathbf{R}}$ has sufficiently negligible cross-correlation: $\mathbf{A}_N \approx \mathbf{I}_{N \times N}$.
- II. The auto-correlations of $\hat{\mathbf{R}}$ are exponentially decreasing, i.e., $\{B_T\}_{ij} = b^{|i-j|}$, with $|b| < 1$.²

Under the two assumptions, we can conduct spectrum analysis of the simplified model, and thus $\rho_T(b)$ is capable of being computed. The major steps are briefly given as follows:

- 1) The mean spectral density can be derived from the Green's function $G(z)$ by using the Sokhotsky's formula:

$$\rho_T(\lambda) = -\frac{1}{\pi} \lim_{\varepsilon \rightarrow 0^+} \text{Im} G(\lambda + i\varepsilon). \quad (10)$$

- 2) The Green's function $G(z)$ can be obtained from the moments' generating function $M(z)$:

$$G(z) = \frac{M(z) + 1}{z}, \quad |z| \neq 0. \quad (11)$$

²This is equivalent to modeling residues as an AR(1) process: $\hat{R}_{it} = b\hat{R}_{i,t-1} + \xi_{it}$, where $\xi \sim \mathcal{N}(0, 1 - b^2)$ so that the variance of \hat{R}_t is 1.

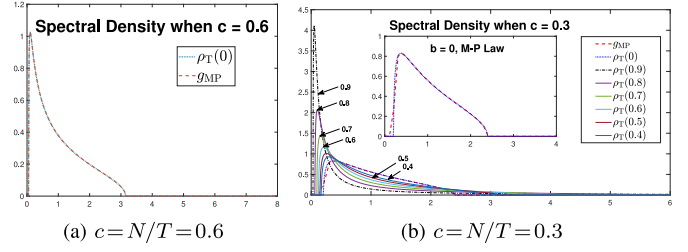


Fig. 3. Spectral Density of $\rho_T(b)$ and g_{MP} .

- 3) $M(z)$ can be found by solving the polynomial equation:

$$a^4 c^2 M^4 + 2a^2 c(-1 + b^2)z + a^2 c) M^3 + ((1 - b^2)^2 z^2 - 2a^2 c(1 + b^2)z + (c^2 - 1)a^4) M^2 - 2a^4 M - a^4 = 0^7 \quad (12)$$

where $a = \sqrt{1 - b^2}$, and $c = \frac{N}{T}$.

It is worth mentioning that when $b = 0$, Assumptions I & II imply that $\hat{\mathbf{R}}$ is a standard Gaussian matrix with i.i.d. random elements, and its spectral density is marked as $\rho_T(0)$. On the other side, Marchenko-Pastur Law says that for a Laguerre unitary ensemble (LUE) matrix $\Gamma \in \mathbb{C}^{N \times T}$ ($c = N/T \leq 1$), its spectral density $g_{MP}(x)$ does follow M-P Law [31]:

$$g_{MP}(x) = \frac{1}{2\pi c x} \sqrt{(x - s_1)(s_2 - x)}, \quad x \in [s_1, s_2] \quad (13)$$

where $s_1 = (1 - \sqrt{c})^2$ and $s_2 = (1 + \sqrt{c})^2$.

The two spectral densities should be equivalent, i.e. $\rho_T(0)$ is equivalent to g_{MP} . Fig. 3 displays this phenomenon.

Fig. 3(b) also tells that the theoretical spectral densities $\rho_T(b)$ are distinguishable with different coefficients b in the AR model. This property implies that the (latent) coefficients b offers excellent potential for the metric space construction. With the help of metric space, the randomness component of the observed data is able to be addressed via spectrum analysis.

E. Metric Space Designing

To design a metric space for solving the mentioned match problem, we need to assign a set and then define a distance function (metric) on it. What we have in practice are the observed data \mathbf{Z}_{ob} in the form of multiple time-series, and SE outputs $\hat{\mathbf{Z}}_m$ derived from \mathbf{Z}_{ob} and Model M_m . The difference (Eq. 1: $\mathbf{X}_m = \mathbf{Z}_{ob} - \hat{\mathbf{Z}}_m$) is the first and most obvious choice for us to extract some statistical information from.

Before designing the metric space, let us look through those conventional statistics indicators, e.g., first/second moment (mean/variance). We have already argued that the profiles of renewables-derived uncertainties do follow AR models. Mean and variance contain enough statistical information for an i.i.d. Gaussian random variable, but insufficient for an AR model, not to mention multiple AR processes (temporal aspect) on those connected distributed access points (spatial aspect).

Some more powerful tools are needed to map the difference \mathbf{X}_m , which consists of a large number of random variables, into some indicator within a well designed metric space. The proposed hybrid framework (Fig. 1) conducts jointly temporal-spatial analysis of \mathbf{X}_m as follows: First, \mathbf{X} is converted

into \mathbf{R} with a given p (Eq. 7), and then the ESD ρ_E is calculated (Eq. 9). On the other hand, with a given coefficient b , the theoretical spectral density $\rho_T(b)$ is capable of being computed (Eq. 8 \rightarrow 12 \rightarrow 11 \rightarrow 10). Then, the metric distance such as Jensen-Shannon divergence can be naturally studied:

$$d(\mathbf{Z}_{\text{ob}}, \hat{\mathbf{Z}}_m) = |\mathbf{X}_m|_{\mathcal{D}} = \mathcal{D}(\rho_T(b), \rho_E(p)) = \sum_i p_i \mathcal{D}_{\text{JS}}(a_i, b_i) \quad (14)$$

where $\mathcal{D}_{\text{JS}}(a, b) = a \log a + b \log b - 2v \log v$ with $v = \frac{a+b}{2}$.

With the metric space design, the TI task is converted into a convex optimization problem

$$\arg \min_m d(\mathbf{Z}_{\text{ob}}, \hat{\mathbf{Z}}_m) = \arg \min_m \mathcal{D}(\rho_T(b), \rho_E(p)). \quad (15)$$

The convex optimization can be readily calculated using modern software toolbox such as CVX.

V. CASE STUDIES

A. Case Background and Model Bank

IEEE 33-bus Network (Fig. 2) is used to validate our proposed hybrid framework. Considering a sampling dataset with 1440 observations (4 hours with a 0.1 Hz sampling rate). This observation leads to the empirical dataset \mathbf{Z}_{ob} , which consists of local sample data from 33 access points. Following Section II-A, it is assumed that there is no prior information about the power flow on the connected branch ($P_{i,j}$ and $Q_{i,j}$).

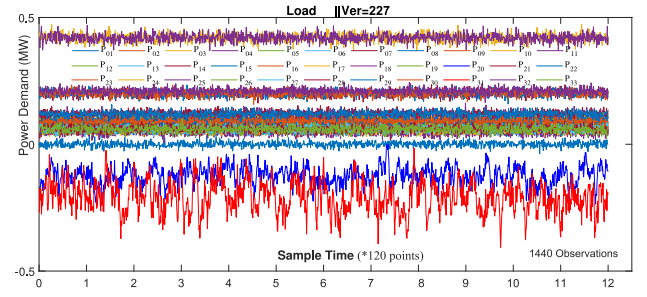
Fig 4(a) depicts the active power generation/consumption at each node ($P_i \in \mathbf{P}_{\text{ob}} \subset \mathbf{Z}_{\text{ob}}$). For Node 20 and Node 31, the curves are of high variation derived from the behavior of some wind speed data in practice. For other nodes, however, the curves are stationary since the profile of routine power usages is relatively smooth. It is noteworthy that we only discuss the randomness component as mentioned in Section II.

The physical grid only has numerous possible operation models (Section III-C), and we arrange them to form the model bank (Fig 5). Through parallel PF analysis, we test each model, e.g. Model M_m , and work out its SE result $\hat{\mathbf{Z}}_m$. Fig 4(b) depicts the voltage magnitudes of Model M_1 ($\hat{\mathbf{V}}_1 \subset \hat{\mathbf{Z}}_1$).

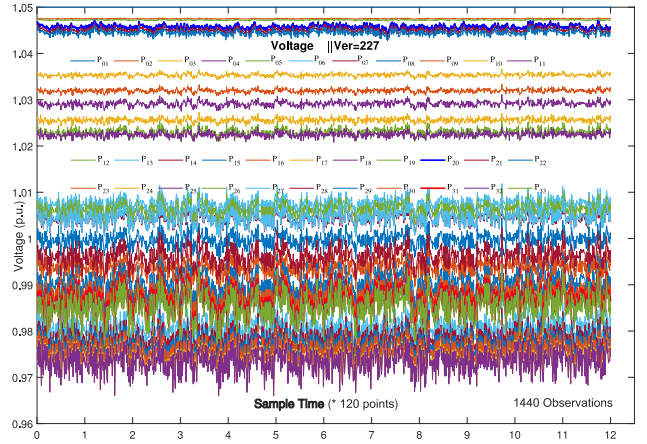
The low-dimensional statistics Mean μ and Variation σ contain enough statistical information about Gaussian variables, but not about the renewables-derived randomness $\hat{\mathbf{V}}_1$, of which multiple AR time-series contribute a major part. Moreover, Mean μ is vulnerable to fixed measurement error. To address those renewables-derived uncertainties is the primary motivation for our proposed framework.

B. Case Designing

We assume that at time point $t = 720$, due to some reason there is an operation model transformation from Model M_1 to M_2 —the system operates under M_1 during $0 \sim 720$, and M_2 during $721 \sim 1440$. We also take the measurement error into account, and regard it as a Gaussian random variable E , whose statistical properties can be fully described by mean μ_E and standard deviation σ_E .



(a) \mathbf{P}_{real} : Load Behavior in IEEE 33-bus Network



(b) $\hat{\mathbf{V}}_1$: Voltage Magnitude of Model 1

Fig. 4. Dataset from 33 Points and 1440 Observations.

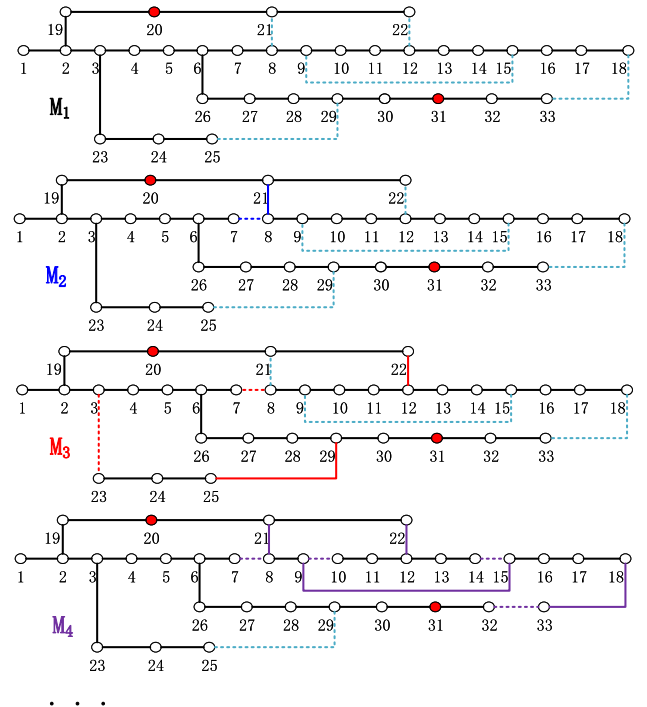


Fig. 5. Models Stored in the Model Bank.

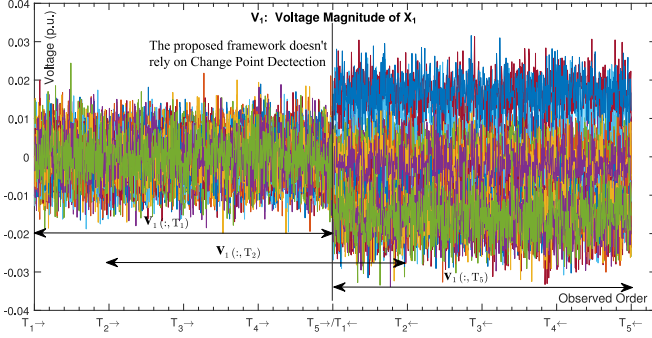


Fig. 6. \mathbf{V}_1 : Voltage Magnitude Component of Difference \mathbf{X}_1 .

Our previous work [32] has already shown that the fixed measurement error μ_E has no influence to the RMT-based analysis and indicator at all. Therefore we only need to consider σ_E . Referring to [33], it is supposed that $\sigma_E = 0.005$ p.u.—the standard deviation of the measurement errors is 0.5%. The uncertainties caused by renewables and measurement errors together may significantly influence the statistical properties of observed data, thereby disabling TI performance.

When both \mathbf{Z}_{ob} , the observed data, and $\hat{\mathbf{Z}}_m$, the SE output of Model M_m , are known a priori, so is their difference \mathbf{X}_m . As the reasons given in our previous work [20], only voltage magnitude $\mathbf{V}_m \subset \mathbf{X}_m$ is discussed. Furthermore, we keep each observation duration 720 sampling points, and thus divide the whole observation into 5 periods: T_1 (1 ~ 720), T_2 (181 ~ 900), T_3 (361 ~ 1080), T_4 (541 ~ 1260), and T_5 (721 ~ 1440). We use $\mathbf{V}_m(:, T_j)$ to represent the voltage difference on all the 33 nodes during T_j , which can be denoted as \mathbf{V}_{m_j} when there is no ambiguity. Fig. 6 shows the voltage magnitude difference in each period for Model M_1 : $\mathbf{V}_{1_1}, \mathbf{V}_{1_2}, \dots, \mathbf{V}_{1_5}$.

C. Regression-Based TI and its Failure When Uncertainties are Not Well Addressed

We test the TI performance by employing Jacobian matrix \mathbf{J} (Eq. 5), a matrix variate which is strongly associated with network topology \mathbf{Y} . From Eq. (4), the estimation of \mathbf{J} can be naturally formulated as a regression problem. Under fairly general conditions, the target \mathbf{J} , according to Eq. (3), keeps nearly constant within some duration, called Δt , due to the stability of the system, or concretely, of variables V, θ, Y . During Δt , considering T times observation at time instants t_i , ($i = 1, 2, \dots, T, t_T - t_1 = \Delta t$), we acquire the operation data points in the form of $(\mathbf{x}^{(i)}, \mathbf{y}^{(i)})$.

In this case, we take the period T_1 (1 ~ 720) for study. The truth-value of \mathbf{J} on each sampling point is calculated via Eq. (3) in a model-based way. The result validates that \mathbf{J} indeed keeps nearly constant at around its mean \mathbf{J}_{Mean} (Fig. 7(a), 20 level), and with the standard deviation \mathbf{J}_{SD} (Fig. 7(b), 0.04 level). Therefore, it is reasonable to set \mathbf{J}_{Mean} as the benchmark during this observation period T_1 .

Defining $\Delta \mathbf{x}^{(k)} \triangleq \mathbf{x}^{(k+1)} - \mathbf{x}^{(k)}$ and $\Delta \mathbf{y}^{(k)} \triangleq \mathbf{y}^{(k+1)} - \mathbf{y}^{(k)}$, Eq. (4) is rewritten as $\Delta \mathbf{y}^{(k)} \approx \mathbf{J}^{(k)} \Delta \mathbf{x}^{(k)}$. Since \mathbf{J} keeps nearly

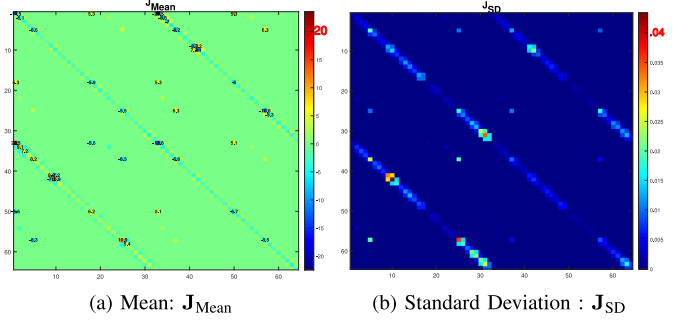


Fig. 7. Basic Statistical Information of \mathbf{J} in Period T_1 .

constant during T_1 , the expression is reformulated as

$$\mathbf{B} \approx \mathbf{J} \mathbf{A} \quad (16)$$

where $\mathbf{J} \in \mathbb{R}^{K \times K}$, $\mathbf{B} = [\Delta \mathbf{y}^{(1)}, \dots, \Delta \mathbf{y}^{(T)}] \in \mathbb{R}^{K \times T}$, and $\mathbf{A} = [\Delta \mathbf{x}^{(1)}, \dots, \Delta \mathbf{x}^{(T)}] \in \mathbb{R}^{K \times T}$.

The least square method is the first and the most obvious choice as the solution to the regression problem formulated as Eq. (16). It is capable of handling the scenarios where the network topologies \mathbf{Y} are unreliable or even totally unavailable, and thus, \mathbf{Y} are no longer essential information. This property agrees with our assumption in Section II-A. Conversely, the result of \mathbf{J} estimation inherently contains the most up-to-date information about \mathbf{Y} .

In particular, ordinary least square (OLS) and total least square (TLS) [34] are tested, and numerous scenarios with different types of noise are studied. Fig. 8 shows the results.

- 1) Fig. 8(a) and 8(e) tell that both OLS and TLS perform well (\mathbf{J}_{Err} is at the same order as \mathbf{J}_{SD} ; \mathbf{J}_{Err} —difference between the estimated values and the benchmark \mathbf{J}_{Mean}) when there is no error on neither \mathbf{y} side (\mathbf{B} in Eq 16) nor \mathbf{x} side (\mathbf{A}).
- 2) Fig. 8(b) and 8(f) tell that their performances reduce from good level to acceptable level when some Gaussian error (5%) injects into \mathbf{y} (\mathbf{x} is assumed to be error free).
- 3) Fig. 8(c) and 8(g) tell that when the Gaussian error (5%) comes from both \mathbf{y} and \mathbf{x} , TLS becomes the only option to reach a barely-passing result. TLS is a type of error-in-variables regression, a least squares data modeling technique in which observational error on both dependent and independent variables is taken into account [35].
- 4) However, if the noise does not follow i.i.d. Gaussian distribution, as the aforementioned renewables-derived uncertainties, both OLS and TLS fail in this kind of regression task. These uncertainties, which are analytically intractable under conventional framework, will almost certainly lead to bad results without a proper treatment, as illustrated in Fig. 8(d) and 8(h). This is the primary motivation for our proposed hybrid framework.

D. Elementary RMT-Based Analysis

To make these renewables-derived uncertainties analytically tractable, we have to study the problem in a high-dimensional

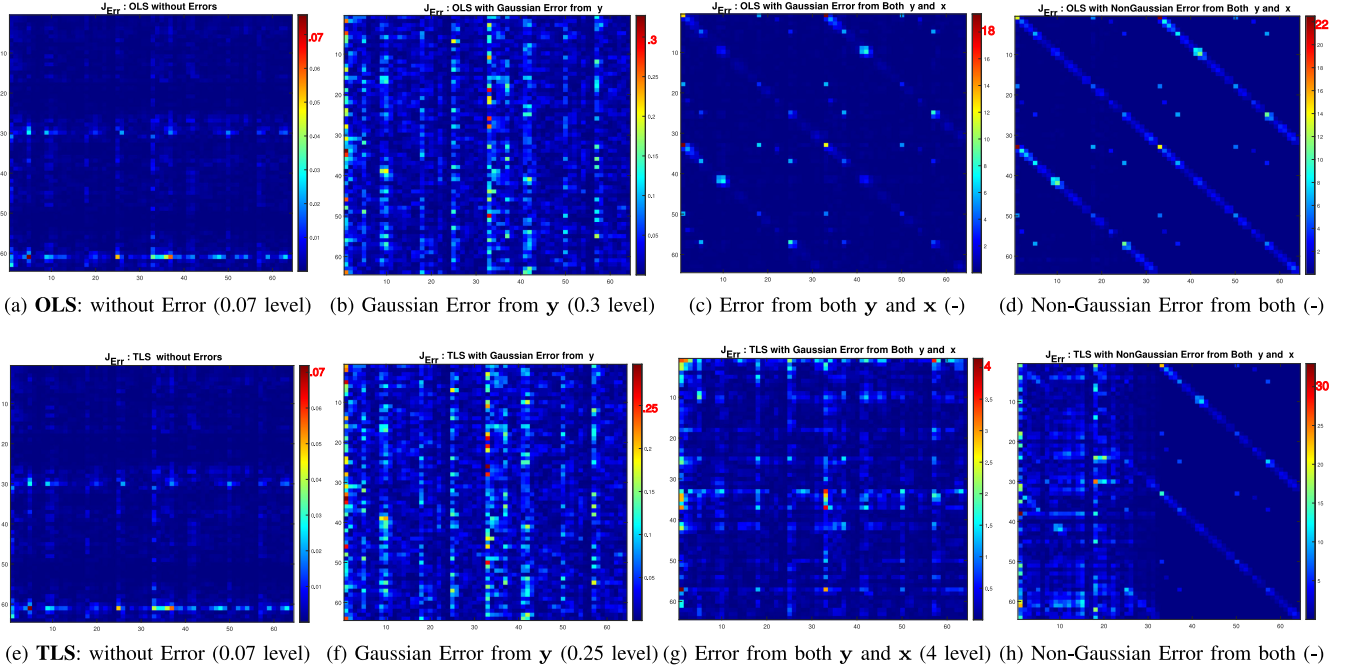


Fig. 8. Performance of OLS and TLS on \mathbf{J} Estimation with Different Types of Noise.

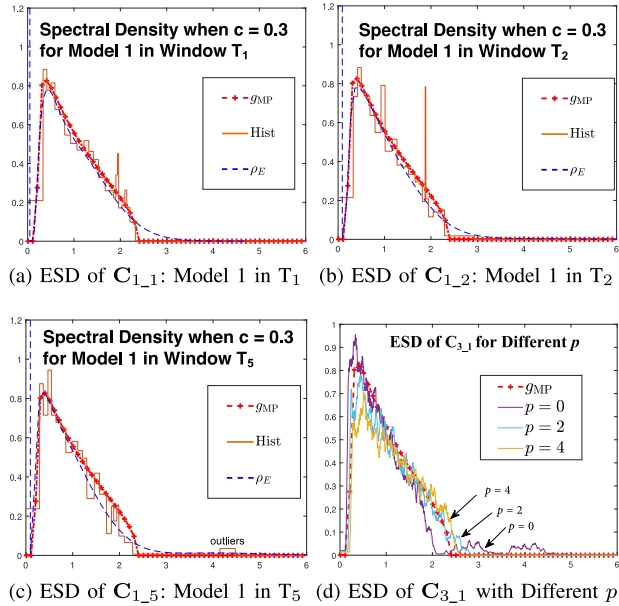


Fig. 9. ESD of \mathbf{C}_{m_j} for Model m in Period T_j .

space. Under the RMT framework provided in our previous work [20], we gain insight the uncertainties from the spectrum aspect via high-dimensional analysis.

Fig. 9 depicts the analysis result for Model M_m in Period T_j . The ‘ g_T ’ Curve is the theoretical M-P Law spectral density as given in Eq. (13). The ‘Hist’ Curve means histogram for the ESD. First, we set factor numbers p in Eq. (7) to convert difference \mathbf{V} into residues \mathbf{R} . Then we calculated the ESD of $\mathbf{C}_{m_j} = \frac{1}{T} \mathbf{R} \mathbf{R}^T$ according to Eq. (9). The ‘ ρ_E ’ Curve is the

probability density estimate of the ‘Hist’ Curve using Kernel Smoothing Function (code ‘ksdensity(·)’ in Matlab, for Model M_1) or Moving Average Function (code ‘smooth(·)’, for M_3).

The metric space designed in Section IV-E enables us to quantify the TI performance of each bank model in spectrum space. The outliers tend to large and evident as the corresponding model becomes deviant, and the deviation will lead to a large $d(\mathbf{V}_{ob}, \hat{\mathbf{V}}_{m_j}) = |\mathbf{V}_{m_j}|_{\mathcal{D}}$ as defined in Eq. (14).

E. FA Analysis and Time-Series Analysis

For each difference-derived random matrix, e.g. \mathbf{V}_{3_1} , we calculate its ESD with a different factor numbers p , and then obtain the results as shown in Fig. 9(d). As we increase factor numbers p , the outliers are alleviated. This phenomenon agrees with the fact that FA is often used for dimension reduction in sampling data with underlying constructs, i.e. converting \mathbf{V}_{m_j} into $\mathbf{L}^{(p)} \mathbf{F}^{(p)}$ following Eq. (7). However, the residues part \mathbf{R}_{m_j} could also have some latent construct. For instance, the randomness caused by a wind following AR model with coefficients b . This statistic property cannot be eliminated simply by increasing p . Fortunately, Ref. [27] applies RMT to derive spectral density of large sample covariance matrices generated by multivariate ARMA processes in analytic forms (Eq. 8→12→11→10). Following Ref. [27], we push forwards our research on the residues \mathbf{R}_{m_j} .

Temporal analysis is conducted first by estimating the auto-correlation coefficient b of \mathbf{R}_{m_j} using Burg’s method (code ‘arburg(·)’ in Matlab). If the picked model perfectly matches the real grid, the renewables-derived auto-correlation would be eliminated, and only (Gaussian) measurement error remains. Fig. 10 validates this—all the nodes on \mathbf{V}_{1_1} (Column C_1) and

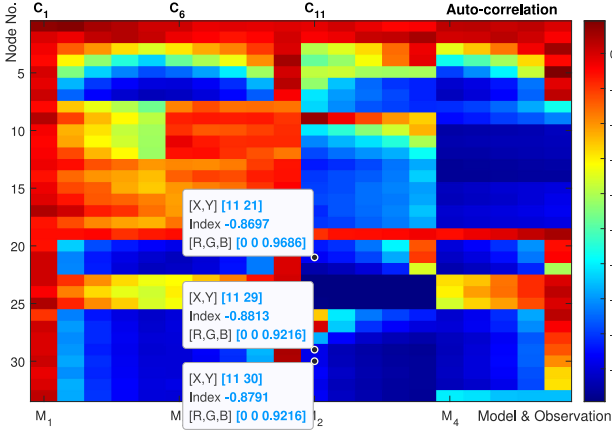


Fig. 10. Estimated auto-correlation coefficient \hat{b} of \mathbf{V}_{m-j} .

\mathbf{V}_{2-5} (C_{10}) are of small auto-correlation ($\hat{b} \approx 0$), and therefore we should accept the hypothesis that Model M_1 matches the real system in Period T_1 , and M_2 in Period T_5 .

Fig. 9(a) also depicts the phenomenon that only measurement error remains— \mathbf{V}_{1-1} -derived ESD does closely match the theoretical ‘ g_T ’ Curve (M-P Law) and no obvious outliers exist. Besides, we can find that the values of the nodes close to the reference bus (e.g. Node 2, 3, 19) are usually stable around 0. The phenomenon that these nodes are insusceptible to renewables is consistent with our common sense.

F. Jointly Temporal-Spatial Analysis With Latent Structure

M-P Law can nicely model \mathbf{R}_{1-1} in some sense. Then some open questions are raised, for example: 1) How to model other columns, e.g., Column 11 (\mathbf{R}_{3-1})? 2) Can we extract some information from them, and how? To address these questions, jointly temporal-spatial analysis is discussed.

We revisit our prior information to find out the causes which may decide/influence the statistical properties of \mathbf{R}_{m-j} . One major cause is the two independent renewables on Node 20 and Node 31. From the local field data we know that their power outputs follow AR process with some latent structure. Another major cause is the inherent topology \mathbf{Y} , although it is unknown and may have a transformation at some time point.

Then we conduct the analysis with the data from a few nodes but not all of them. This is practical when the advanced sensors such as μ PMUs are only deployed on some important buses. RMT-framework inherently supports statistical analysis with data only from a subset of nodes—the data matrix can be naturally divided into data blocks without additional error, but this is not true for mechanism models. Our previous work [32] gives a discussion on this RMT-framework property.

For Column 11 (\mathbf{R}_{3-1}), we take the renewables-influenced nodes’ data ($b \approx 0.9$) into account, and then make a jointly temporal-space analysis following Section IV. The coefficients \hat{b} of these influenced nodes are similar. With the prior knowledge of Model M_3 stored in the bank, we divide these influenced nodes into three parts: 1) Node 6, 7; 2) Node 20~22; and

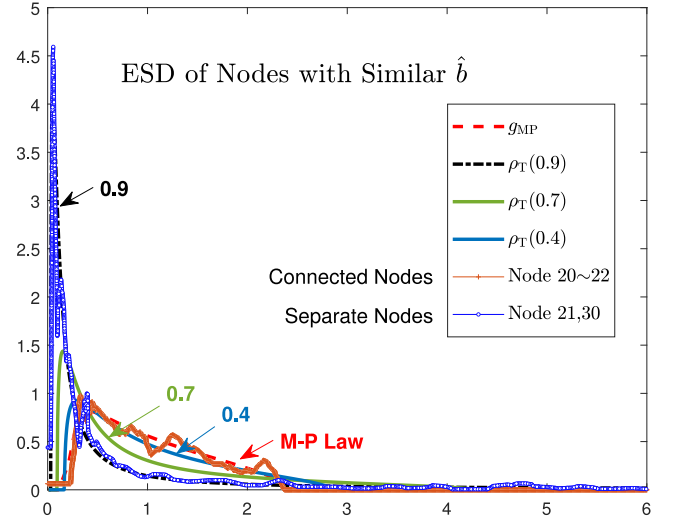


Fig. 11. Jointly Spatial-temporal Analysis to Grid Nodes.

3) Node 29~33. Then we study their cross-correlation under this division—the closely connected nodes must show strong correlation, while the separated nodes show the independence. Based on this property, we use the theoretical spectral density $\rho_T(b)$ to test them, and the results are given in Fig. 11.

The ESD of relevant data derived from separated nodes closely matches the theoretical density $\rho_T(0.9)$. This phenomenon is built upon the premise of the Assumption I in Section IV-D ($\hat{\mathbf{R}}$ has sufficiently negligible cross-correlation: cross-covariances matrix $\mathbf{A}_N \approx \mathbf{I}_{N \times N}$). It means that the randomness component of these separated nodes are influenced by renewables with independent behaviors. This independence is often reasonable especially for an integrated energy system (IES) with diverse sources. While for those closely connected nodes (Node 20~22 in this case), the independence condition is violated, so there is no consistency between ρ_E and $\rho_T(0.9)$.

G. Test With IEEE 85-bus Network

In addition, we test our framework using IEEE 85-bus radial distribution systems. The sampling sensors, renewable generators with diverse/similar patterns are deployed as Fig. 12.

As a distribution grid usually operates in open loop, we just test the pair switch of the normally closed branches and the normally open branches. In particular, we test the pair switch of the normally closed branches B_{11-12} (closed→open) companied with the normally open branch B_{44-84} (open→closed) in Model M_2 , and with B_{66-83} (open→closed) in M_3 , respectively. The error of branch impedance is also tested— M_4 tests B_{5-18} , B_{9-10} , B_{60-63} , B_{32-40} , and B_{35-48} . Similar to Fig. 10 and 11, Fig. 13 a shows the time-series information, and Fig. 13(b) shows the jointly spatial-temporal analysis results.

The results in Fig. 13 validate the hybrid framework again. This framework is suitable to the scenarios when the renewables-behavior dominates our observed data. For the nodes influenced by multiple sources, such as Node 25~32, however, it is hard to model them in practice. Under an ideal scenario, independent

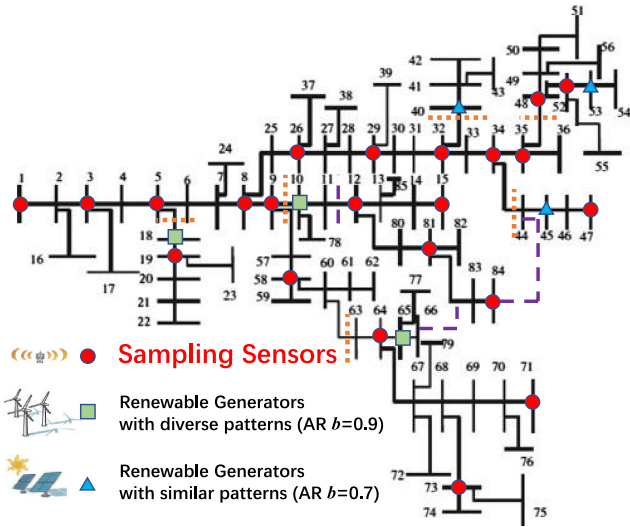
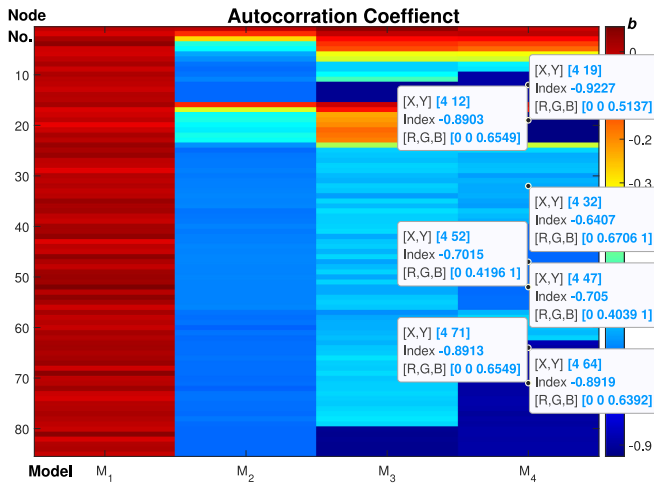
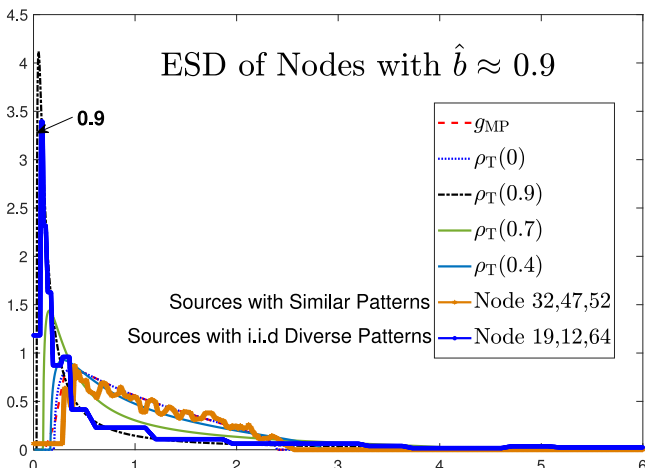


Fig. 12. IEEE 85-bus radial distribution systems.



(a) Estimated auto-correlation coefficient \hat{b} of \mathbf{V}_m



(b) Jointly Spatial-temporal Analysis

Fig. 13. Result of IEEE 85-bus Radial Distribution Systems.

component analysis (ICA) or free component analysis (FCA) [36] may be applied to separate the mixed signal into additive (independent) subcomponents. The combination of ICA/FCA and our framework offers excellent potential for a more complex scenario.

VI. CONCLUSION

This paper explores several high-dimensional analytics in the context of topology identification. We propose a hybrid framework, by tying AR model, FA, and RMT together, to handle the renewables-derived uncertainties in the form of multiple time-series. Our framework, through a systematic and theoretical procedure, makes these uncertainties analytically tractable, and is immune to fixed measurement error.

Several future studies are in order. Clearly, further research is needed to employ the more general residue modeling, for which we can calculate the spectral density readily. For example, as described in [27], if considering vector ARMA(1,1) processes, we have up to 6th-order polynomial equations. Obviously, compared to i.i.d. Gaussian noise, the joint temporal model (AR) and spatial model (FA) oftentimes provide more flexible and rigorous models and analyses on renewables-derived uncertainties. Besides, the framework is capable of handling comprehensive behavior (on the nodes influenced by multiple sources) with the help of existing algorithm such as ICA. The combination of conventional tasks in power system with novel tools in data science is a long-term goal in our community, especially in big data era. In addition, this hybrid framework can be extended to an integrated energy system, in which randomness and independence is more evident.

REFERENCES

- [1] F. F. Wu and W. H. E. Liu, "Detection of topology errors by state estimation power systems," *IEEE Trans. Power Syst.*, vol. 4, no. 2, pp. 50–51, Feb. 1989.
- [2] S. Bolognani, N. Bof, D. Michelotti, R. Muraro, and L. Schenato, "Identification of power distribution network topology via voltage correlation analysis," in *Proc. 52nd IEEE Conf. Decis. Control*, 2013, pp. 1659–1664.
- [3] G. Cavraro and V. Kekatos, "Graph algorithms for topology identification using power grid probing," *IEEE Control Syst. Lett.*, vol. 2, no. 4, pp. 689–694, Oct. 2018.
- [4] D. Deka, S. Backhaus, and M. Chertkov, "Structure learning in power distribution networks," *IEEE Trans. Control Netw. Syst.*, vol. 5, no. 3, pp. 1061–1074, Sep. 2017.
- [5] O. Ardakanian *et al.*, "On identification of distribution grids," *IEEE Trans. Control Netw. Syst.*, vol. 6, no. 3, pp. 950–960, Sep. 2019.
- [6] J. Yu, Y. Weng, and R. Rajagopal, "Patopa: A data-driven parameter and topology joint estimation framework in distribution grids," *IEEE Trans. Power Syst.*, vol. 33, no. 4, pp. 4335–4347, Jul. 2017.
- [7] Y. Yuan, S. Low, O. Ardakanian, and C. Tomlin, "Inverse power flow problem," 2016, *arXiv:1610.06631*.
- [8] X. He, L. Chu, R. C. Qiu, Q. Ai, Z. Ling, and J. Zhang, "Invisible units detection and estimation based on random matrix theory," *IEEE Trans. Power Syst.*, vol. 35, no. 3, pp. 1846–1855, May 2019.
- [9] B. Yang, T. Yu, H. Shu, J. Dong, and L. Jiang, "Robust sliding-mode control of wind energy conversion systems for optimal power extraction via nonlinear perturbation observers," *Appl. Energy*, vol. 210, pp. 711–723, 2018.
- [10] R. Singh, E. Manitsas, B. C. Pal, and G. Strbac, "A recursive Bayesian approach for identification of network configuration changes in distribution system state estimation," *IEEE Trans. Power Syst.*, vol. 25, no. 3, pp. 1329–1336, Aug. 2010.

- [11] G. Cavraro and R. Arghandeh, "Power distribution network topology detection with time-series signature verification method," *IEEE Trans. Power Syst.*, vol. 33, no. 4, pp. 3500–3509, Jul. 2018.
- [12] Z. Tian, W. Wu, and B. Zhang, "A mixed integer quadratic programming model for topology identification in distribution network," *IEEE Trans. Power Syst.*, vol. 31, no. 1, pp. 823–824, Jan. 2015.
- [13] R. Qiu and P. Antonik, *Smart Grid and Big Data*. Hoboken, NJ, USA: Wiley, 2015.
- [14] Y. C. Chen, J. Wang, A. D. Domínguez-García, and P. W. Sauer, "Measurement-based estimation of the power flow jacobian matrix," *IEEE Trans. Smart Grid*, vol. 7, no. 5, pp. 2507–2515, Sep. 2016.
- [15] J. Yeo and G. Papanicolaou, "Random matrix approach to estimation of high-dimensional factor models," 2016, *arXiv:1611.05571*.
- [16] X. Ding and F. Yang, "Spiked separable covariance matrices and principal components," 2019, *arXiv:1905.13060*.
- [17] M. He and J. Zhang, "A dependency graph approach for fault detection and localization towards secure smart grid," *IEEE Trans. Smart Grid*, vol. 2, no. 2, pp. 342–351, Jun. 2011.
- [18] Y. Sharon, A. M. Annaswamy, A. L. Motto, and A. Chakraborty, "Topology identification in distribution network with limited measurements," in *Proc. IEEE PES Innovat. Smart Grid Technol.*, 2012, pp. 1–6.
- [19] D. C. Montgomery, C. L. Jennings, and M. Kulahci, *Introduction to Time Series Analysis and Forecasting*. Hoboken, NJ, USA: Wiley, 2016.
- [20] X. He, Q. Ai, R. C. Qiu, W. Huang, L. Piao, and H. Liu, "A big data architecture design for smart grids based on random matrix theory," *IEEE Trans. Smart Grid*, vol. 8, no. 2, pp. 674–686, Mar. 2017.
- [21] P. Bacher, H. Madsen, and H. A. Nielsen, "Online short-term solar power forecasting," *Sol. Energy*, vol. 83, no. 10, pp. 1772–1783, 2009.
- [22] D. D. Suhr, "Principal component analysis vs. exploratory factor analysis," in *Proc. 13th Annu. SAS Users Group Int. Conf.*, 2005, paper 203-30.
- [23] J. Fan, Y. Liao, and M. Mincheva, "High dimensional covariance matrix estimation in approximate factor models," *Ann. Statist.*, vol. 39, no. 6, 2011, Art. no. 3320.
- [24] I. I. Dimov, P. N. Kolm, L. Maclin, and D. Y. Shiber, "Hidden noise structure and random matrix models of stock correlations," *Quantitative Finance*, vol. 12, no. 4, pp. 567–572, 2012.
- [25] M. Pelger, "Large-dimensional factor modeling based on high-frequency observations," *J. Econometrics*, vol. 208, no. 1, pp. 23–42, 2019.
- [26] X. Shi, R. Qiu, Z. Ling, F. Yang, H. Yang, and X. He, "Spatio-temporal correlation analysis of online monitoring data for anomaly detection and location in distribution networks," *IEEE Trans. Smart Grid*, vol. 11, no. 2, pp. 995–1006, Mar. 2020.
- [27] Z. Burda, A. Jarosz, M. A. Nowak, and M. Snarska, "A random matrix approach to Varma processes," *New J. Phys.*, vol. 12, no. 7, 2010, Art. no. 075036.
- [28] A. Gomez-Exposito, A. J. Conejo, and C. Canizares, *Electric Energy Systems: Analysis and Operation*. Boca Raton, FL, USA: CRC press, 2018.
- [29] T. Rogers, "New results on the spectral density of random matrices," Ph.D. dissertation, King's College London, London, U.K., 2010.
- [30] L. Zhang, "Spectral analysis of large dimensional random matrices," Ph.D. thesis, Nat. Univ. Singapore, Singapore, 2006.
- [31] V. A. Marčenko and L. A. Pastur, "Distribution of eigenvalues for some sets of random matrices," *Sbornik: Math.*, vol. 1, no. 4, pp. 457–483, 1967.
- [32] X. He, R. C. Qiu, Q. Ai, L. Chu, X. Xu, and Z. Ling, "Designing for situation awareness of future power grids: An indicator system based on linear eigenvalue statistics of large random matrices," *IEEE Access*, vol. 4, pp. 3557–3568, 2016.
- [33] X. Ma, W. Li, G. Yu, R. Cao, Q. Zhang, and X. Zhang, "Development of high voltage ac energy meter," in *Proc. Conf. Precis. Electromagn. Meas.*, 2012, pp. 132–133.
- [34] F. Passerini and A. M. Tonello, "Power line network topology identification using admittance measurements and total least squares estimation," in *Proc. IEEE Int. Conf. Commun.*, 2017, pp. 1–6.
- [35] Wikipedia, "Total least squares," 2018. [Online]. Available: https://en.wikipedia.org/wiki/Total_least_squares
- [36] H. Wu and R. R. Nadakuditi, "Free component analysis: Theory, algorithms & applications," 2019, *arXiv:1905.01713*.